Proceedings of The Thirteenth (2003) International Offshore and Polar Engineering Conference
Honolulu, Hawaii, USA, May 25−30, 2003

ISBN 1−880653-60−5 (Set); ISSN 1098−6189 (Set)

On Aerodynamic Characteristics of a Hybrid-Sail with Square Soft Sail

Toshifumi Fujiwara, Koichi Hirata, Michio Ueno and Tadashi Nimura
National Maritime Research Institute
Tokyo, Japan

ABSTRACT

It is a matter of concern on environmental problems all over the world to reduce exhaust of carbon dioxide gas (CO_2) assumed to be one of causes of global warming. We consider that it is one of the important points to decrease the ship's exhaust as the contribution of reduction of CO_2. Some sail-equipped motor ships were constructed in Japan from the viewpoint of reduction on fuel consumption of a ship when the fuel price soared about 20 years ago (Ishihara, 1980; Matsumoto, 1982). In this time, the development of the high performance sail-equipped motor ship that uses clean energy as thrust of the ship is expected to reduce exhaust of CO_2 in environmental problems.

In our research institute, the investigation of aerodynamic characteristics on a hybrid-sail consisted of the rigid wing sail, which plays the role of a mast, a slat and a square soft sail was carried out at the wind tunnel in order to know performances and advantages of a sail-equipped motor ship. As a result the hybrid-sail presented in this paper is very useful compared with the previous sails and equipped on the deck of a motor ship actually. The performance of aerodynamic characteristics is also confirmed by calculation results of CFD.

KEY WORDS: Hybrid-sail; Aerodynamic characteristic; Wind tunnel; Experimental result; CFD calculation; Environmental problem.

INTRODUCTION

The environmental destruction according to global warming in the entire earth is worried because a large amount of use of the fossil fuel increases CO_2 in the atmosphere. In case of a ship, it will be effective to develop new technology of marine engines in order to reduce the exhaust gas. The thrust system using natural energy that might not make atmosphere dirty is also expected instead of the diesel engines. For instance, the use of the wind, the waves and the solar energy can be enumerated as promotion means. Moreover, the engine using the fuel cell is developed in recent years. It is thought, however, that it is the most effective in the current state to use the force of the wind as thrust of a ship from the viewpoint of energy efficiency. It is examined to increase the thrust by using sails on the deck in this paper.

The idea on use of the wind as the thrust of motor ships had been already presented when the fuel price of a ship soared about 20 years ago in oil crisis. Square rigid sails were installed in ships and the effectiveness of the equipped sail was confirmed in Japan. Afterward, since the fuel price fell, the advantage of the sail decreased in the higher cost of the sail production, maintenance and operation. At present, the only one sail-equipped motor ship is plied in Japan except for small fishing vessels.

Now, a new project to develop the sail-equipped motor ship is planned in Japan. In this stage, the economical viewpoint will be sufficiently included in the making of the sail system to prevent on the environmental destruction by the exhaust gas. In our research institute, various investigations of aerodynamic characteristics on the sails were carried out in the wind tunnel. In this paper the results on the hybrid-sail that is a square form are mainly shown and the performance of the hybrid-sail with a gap are investigated. Finally it is confirmed that CFD calculation is efficient measures to assess the performance of the sails.

The results of the experiments in this paper are also used by Minami et al. (2003) to consider the steady condition on manoeuvring performance of a sail-equipped motor ship.

PREVIOUS EQUIPPED SAILS AND PRESENT HYBRID SAIL

The ships equipped with sails on the deck, which were built about 20 years ago, are shown in Fig.1 (Matsumoto, 1982) and Fig.2 (Usuki, 1985) as examples. The tanker (L_{PP}=66m) shown in Fig.1 has two square rigid sails that the total sail area is 200m^2. The bulk carrier (L_{PP}=152m) shown in Fig.2 also has two square rigid sails that the total sail area is 640m^2. Both sails are a circular arc type with a cloth cover to reduce total weight of the sails. The sail-equipped motor ship was also examined in Denmark in recent years (Hansen, 2000).

In this time, high performance of the aerodynamic characteristics for the sail is expected rather than that of those square rigid sails shown in Fig.1 and Fig.2 in smaller costs. Although detailed examinations are more necessary, one idea of the equipped sail is shown in Fig.3. The sail consists of the rigid wing sail of NACA0030 form as a mast, the slat of a circular arc in front of the rigid sail, which controls an air flow

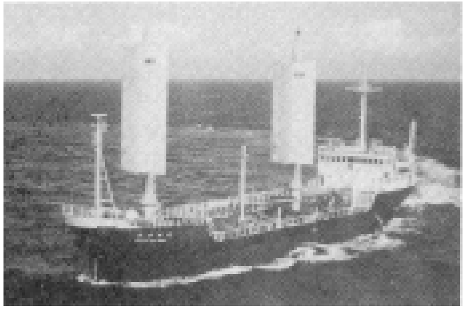

Fig.1 View of the sailing ship 'Shin Aitoku Maru'

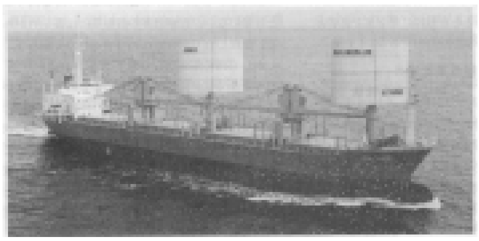

Fig.2 View of the sailing ship 'USUKI PIONEER'

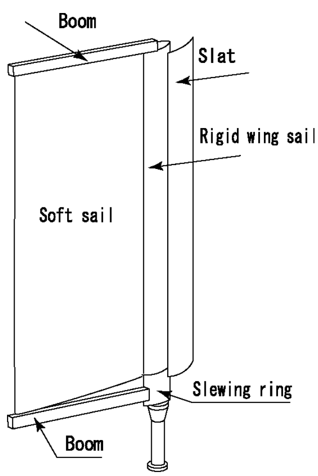

Fig.3 Basic concept of the high performance hybrid-sail

to the rigid sail, and a square soft sale made with a cloth on the edge afterward. At stormy weather, it is assumed that the slat is divided two parts longitudinally and is bended to its half size, and that the soft sale is winded up into the rigid wing sail.

EXPERIMENTS

Experimental models

Fig.4 shows the size of the experimental models. The rigid wing sail of NACA0030 type, which is 1.0m in height and 0.11m in width, was set up on the circle mast that is 0.25m in height. The effect of the boundary layer on the floor can be ignored because the sail is on the circle mast. The chord length and the circular arc radius of the slat are 0.1m respectively. The position of the slat is not translated but the angle of

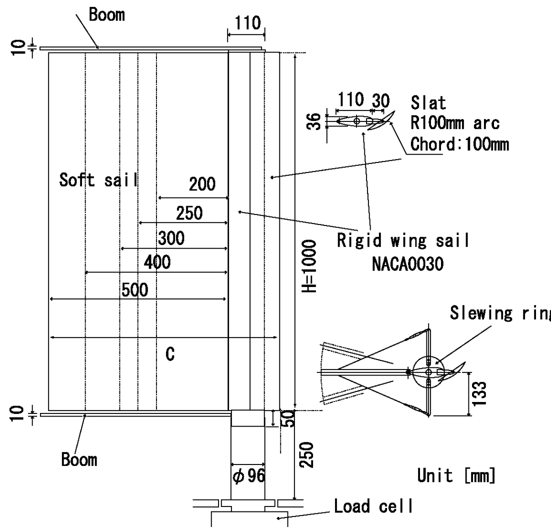

Fig.4 Experimental models

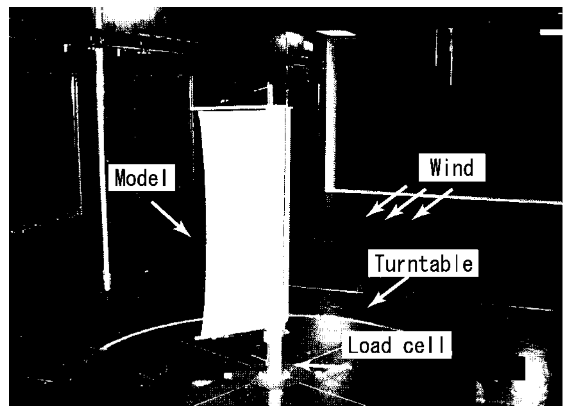

Fig.5 Experimental condition of the model

that against the sail can be changed. The soft sails of 1.0m in height, 0.2, 0.25, 0.3, 0.4, 0.5m in width made with a nylon were used to investigate the effect of aspect ratio.

Experimental condition

The wind tunnel experiments were carried out in our research institute to investigate the aerodynamic characteristics of the sails. The experimental condition is shown in Fig.5. The load cell to measure forces and moment is set up to the center in the turntable and the sail model is jointed on the load cell. The wind velocity is uniform in the vertical direction but there is the boundary layer about 0.1m on the floor in the tunnel.

Wind force and moment coefficients

Fig.6 shows the coordinate system of the model and definitions of the forces and the moment. The forces in the horizontal plane with respect to the wind is the drag force D, positive in the wind direction, and the cross force L, positive to the right when facing into the wind. The moment M for the vertical axis in the X-Y plane is the yawing moment. The α is the angle of the apparent wind based on the rigid wing sail. In the same way, the β and the γ are the slat and the boom angle

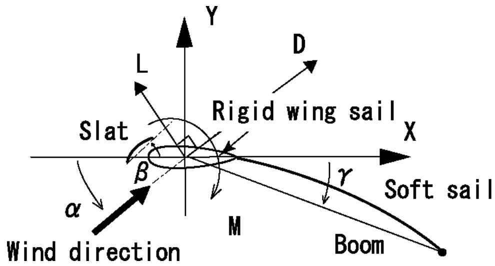

Fig.6 Coordinate system and definitions

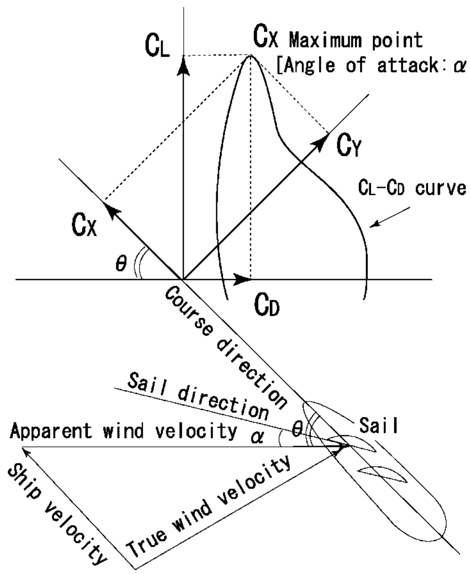

Fig.7 Relationship between the course direction of a ship and the thrust by the wind

respectively.

The lift, drag forces and moment coefficients are defined in non-dimensional form as follows:

$$C_L = L/(1/2\rho_A U^2 S)$$
$$C_D = D/(1/2\rho_A U^2 S) \qquad (1)$$
$$C_M = M/(1/2\rho_A U^2 SC)$$

Here, U; the velocity of wind, ρ_A; the density of air, S; the lateral projected area, C; the chord length.

The chord length C and the lateral projected area S are changed by the slat angle, the wing sail and the soft sail. Here, the S is defined as the sum of the lateral projected area of the wing sail with the slat on the basis of X-axis and the area of the soft sail, that is, the S slightly depends on the slat angle β. The C is obtained from S/H, which the H is the height of the sail as in Fig.4. The aspect ratio (AR) is defined as H^2/S.

The thrust and the side force coefficients C_X, C_Y, which have large influence on the voyage of a ship, are defined as follows:

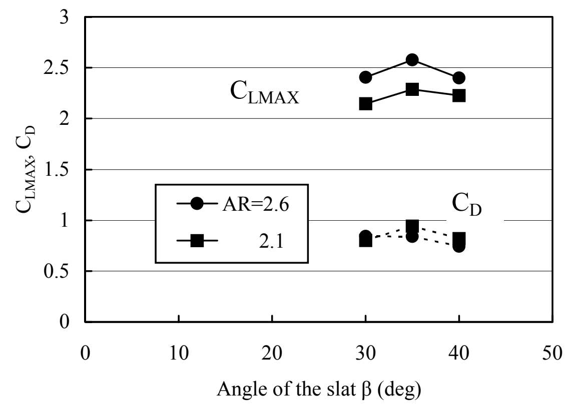

Fig.8 Effect of the slat angle on C_{LMAX} and C_D at C_{LMAX} (γ=30deg)

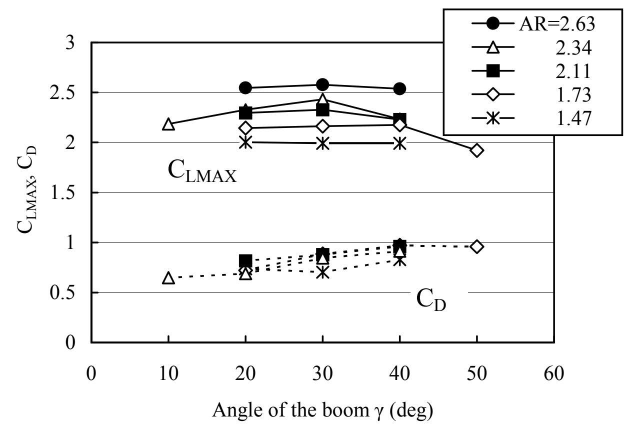

Fig.9 Effect of the boom angle and the aspect ratio on C_{LMAX} and C_D at C_{LMAX} (β=35deg)

$$C_X = C_L \sin\theta - C_D \cos\theta \qquad (2)$$
$$C_Y = C_L \cos\theta + C_D \sin\theta$$

The relationship between course direction of a ship and each wind force coefficient are shown in Fig.7.

Experimental results

All experiments were carried out in U=8m/s, which the Reynolds number used the average chord of the model is about 2×10^5. As shown in Fig.7, the thrust force is mainly decided by the maximum lift (C_{LMAX}) and C_D at C_{LMAX}. First of all, the experimental results of C_{LMAX} and C_D at C_{LMAX} in the various conditions are shown in the figure.

Influence of the slat angle on lift and drag

The experimental results in case that the slat angel β is changed from 30deg to 40deg at the boom angle γ=30deg are shown in Fig.8. The horizontal axis indicates the slat angle and the vertical axis is C_{LMAX} and C_D at C_{LMAX} when the wind direction is changed from 0deg to

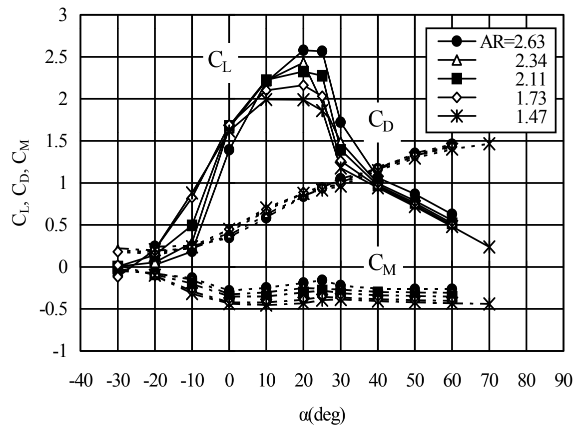

Fig.10 Aerodynamic characteristics of the hybrid sails in the difference of the aspect ratios (β=35deg, γ=30deg)

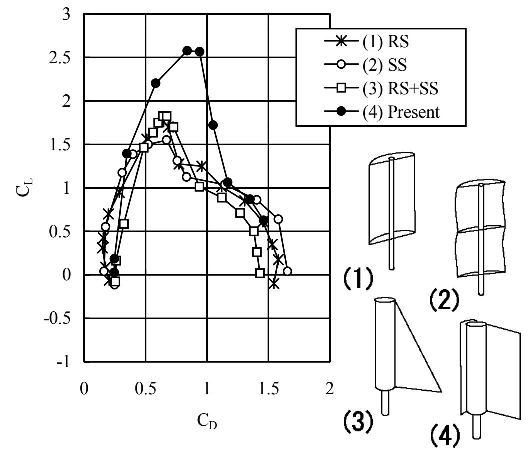

Fig.12 C_L-C_D curve on the present hybrid sail (AR=2.63) and the previous sails (Ishihara,1980)(RS; Rigid Sail, SS; Soft Sail)

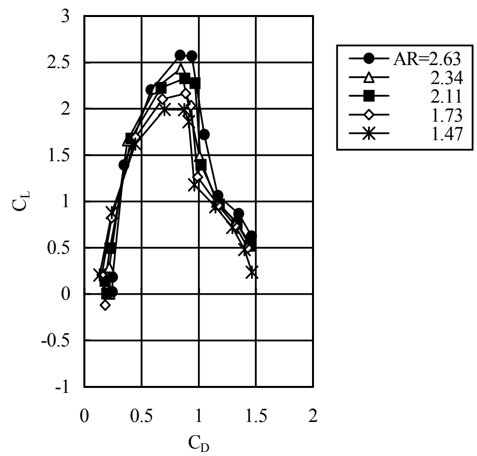

Fig.11 C_L-C_D curve of the hybrid sails (β=35deg, γ=30deg)

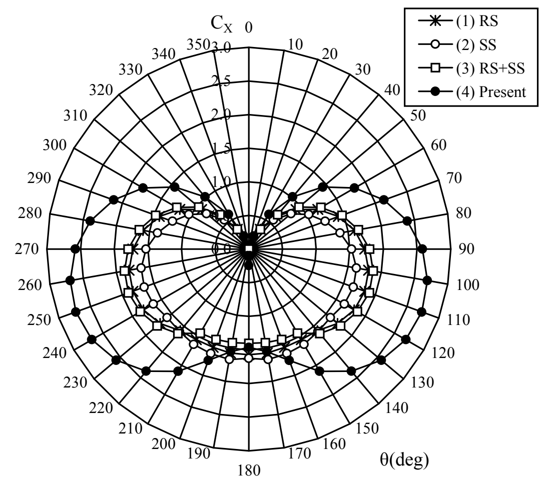

Fig.13 Polar curve on C_X (RS; Rigid Sail, SS; Soft Sail)

90deg. The slat at β=25deg touches with the wing sail. The results of two conditions on the different AR are shown in the figure. It is understood from Fig.8 to be obtained the maximum lift and drag at β=35deg. Even if the aspect ratio is changed, the trend of increase and decrease on C_{LMAX} and C_D seems to be same.

Influence of the boom angle and the aspect ratio on lift and drag

The influence of the boom angle and the aspect ratio on C_{LMAX} and C_D at C_{LMAX} was investigated as shown in Fig.9. The boom angle is in a horizontal axis and C_{LMAX} and C_D are in a vertical axis. The condition of β=35deg was settled to be a standard because the maximum lift was obtained in that slat angle in the Fig.8.

The maximum value of C_{LMAX} is obtained at γ=30deg in the different aspect ratios. The lift coefficients also increase when the aspect ratios increase in the γ=30deg though the change of the drag coefficients in the difference of the aspect ratios is small.

Aerodynamic characteristics on C_L, C_D and C_M

Aerodynamic characteristics on C_L, C_D and C_M in the difference of aspect ratios are shown in Fig.10 in case of the slat angle β=35deg and the boom angle γ=30deg based on the results in Fig.8 and Fig.9. It is understood that the drag coefficient does not change greatly even if the aspect ratio are changed. The lift force coefficient is largely influenced from the aspect ratio. The moment coefficients take negative values in the almost wind directions. The case that the drag coefficient C_D is taken in a horizontal axis is indicated in Fig.11. The conventional wings of high aspect ratio are observed to have the higher lift-curve slopes (Abbott, 1959). In this time, slightly the higher lift-curve slopes are also obtained in case of the high aspect ratio.

Comparison between the present hybrid-sail and the previous sails on the aerodynamic characteristics

Fig.12 shows the comparison between the results of the present sail (AR=2.63, β=35deg and γ=30deg) and those of the previous sails already presented (Ishihara, 1980). No.1 in the figure is the square rigid

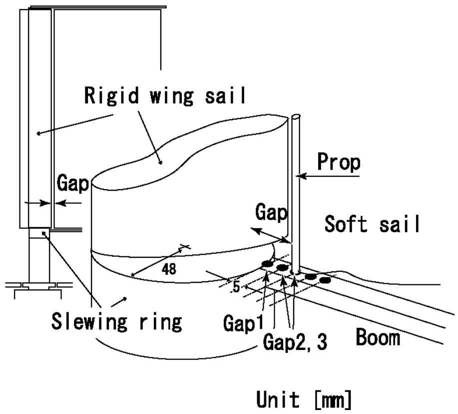

Fig.14 Hybrid-sail with the gap between the rigid wing sail and the soft sail, and position of the prop in the soft sail

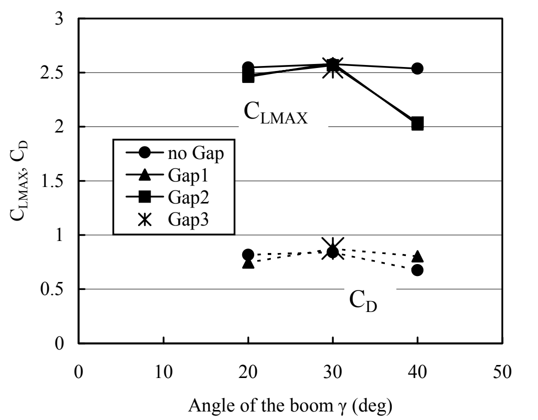

Fig.15 Effect of the boom angle and the gap width on C_{LMAX} and C_D at C_{LMAX} (AR=2.63, β=35deg)

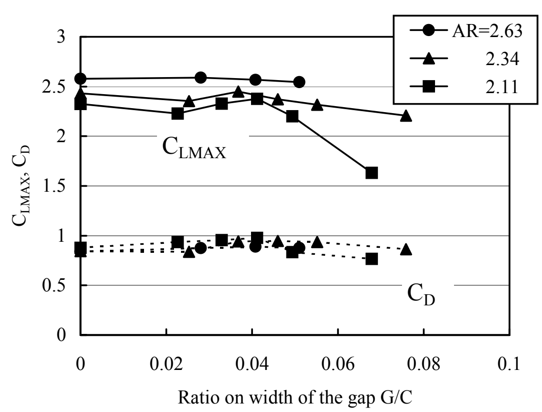

Fig.16 Effect of the gap width and the AR on C_{LMAX} and C_D at C_{LMAX} (β=35deg, γ=30deg)

sail. No.2 is the square soft sail and No.3 is the rigid wing sail with the triangle soft sail. The AR of three kinds of the sails is about 2. The lift coefficient of No.4 proposed in this paper is much larger than that of No.1~3.

It is large difference between No.3 and No.4 to be the slat in front of the sail. Abbott and Doenhoff(1959) show the lift example data of the Clark Y wings with slots and flaps. C_{LMAX} increases about 0.5 in case of the wing with a slat. Fig.12 also shows the similar result. It is understood from the figure that the effect of the slat is very large for the lift force.

Fig.13 shows C_X value at the polar graph on the sails shown in Fig.12. Maximum thrust coefficient of the present sail is about 2.7 in 110deg wind direction. The important point to gain the maximum thrust when 90deg<θ<180deg is that the lift is not only large but the drag is also large as in the equation (2). However, even if the aspect ratio was changed in this experiment results, a big difference was not seen in the drag coefficient either in Fig.10. Therefore, it is necessary to increase the lift coefficient by enlarging the aspect ratio as much as possible to gain the much thrust though it is nature.

The hybrid-sail proposed in this paper is shown to have high performance on the thrust but the mechanism of the sail is a little complex compared with the previous sails. It will become a key point that how it is possible to make it cheaply and simply when actually producing it in the future.

Gap influence between the rigid wing sail and the soft sail

Some separate slats and flaps are ordinarily equipped in the wing of an aircraft because the lift of the wing should be increased when taking off or landing. It is assumed that the control of the exfoliation using the optimum gap and the angle of slats and flaps increases the lift force. A similar idea was applied to the present sail and the aerodynamic characteristics were investigated by using the model. The gap was installed between the rigid wing sail and the soft sail as shown in Fig.14. A thin prop was inserted in the soft sail near side of the rigid wing sail. The position in which the prop was inserted is set from the slewing ring edge to 5mm interval and the influence of the gap widths was investigated.

The experimental results are shown in Fig.15. C_{LMAX} and C_D at C_{LMAX} are shown as same as the previous figure. The lift decreases extremely at γ=40deg having the large gap between the rigid sail and the soft sail. It is understood that interaction between the rigid sail and the soft sail by the flow into the gap has become small.

The influence of the gap and the aspect ratio of the sails is investigated at β=35deg, γ=30deg gained the maximum lift from Fig.15. The results are shown in Fig.16. The experiments were carried out on the conditions of the aspect ratios in 2.11, 2.34, and 2.63 at which the large lift could be obtained. The lift increases by a suitable gap between the rigid sail and the soft sail. This maximum lift point with the gap is larger than that with no gap, but the difference is very small. For the drag coefficients, the gap widths hardly influence on the values.

The phenomenon of increasing on the lift by installing the suitable gap from this experiment was observed. However, the value is very small and it is clarified that the possibility of decreasing the lift is very high. The structure of the sail with the gap will be complicated in producing of a hybrid-sail. It seems that the examination is more necessary to know the effect of the gap in detail if it would be installed in the sail.

CFD CALCULATIONS

When a new type sail is examined like this time, there are many combinations of parts and positions to seek the best performance of the sail, and it is difficult to cover all characteristics of them by the model

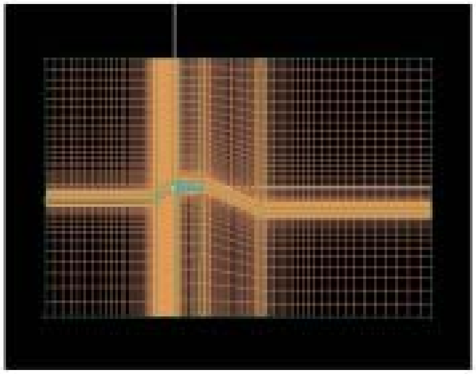

Fig.17 Grid example of the calculation on the hybrid sail
(AR=2.34, β=35deg, γ=20deg)

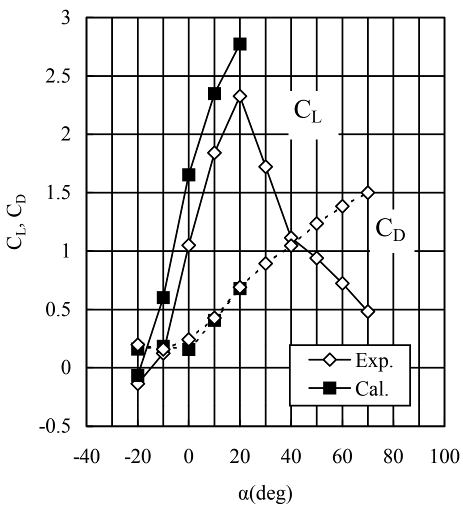

Fig.18 Aerodynamic characteristics of the hybrid sails comparing the calculation results with the experimental ones
(AR=2.34, β=35deg, γ=20deg)

experiments. It is in the current state that examinations of the aerodynamic characteristics can be understood comparatively easily by the CFD calculation. Therefore, the lift and the drag of the square hybrid-sail used in the experiments were calculated to confirm efficiency of the CFD in deciding the specification of the sail, and the results were compared with those of the experiments.

Numerical method

The calculations were carried out by using packaged software 'CFD2000 Storm' supplied by Adaptive Research (1997). 'Storm' is a general-purpose computer program designed to numerically solve the Navier-Stokes equations, which consist of conservation equations for mass, momentum and energy.

Governing equations

The conservation of mass and Newton's second law applied to the fluid passing through a small, fixed fluid volume are expressed as follows:

$$\frac{\partial \rho}{\partial t} + \frac{\partial(\rho u_i)}{\partial x_i} = 0$$
$$\frac{\partial(\rho u_i)}{\partial t} + \frac{\partial(\rho u_i u_j)}{\partial x_j} = \frac{\partial \tau_{ij}}{\partial x_j} - \frac{\partial p}{\partial x_i} + \rho B_i \qquad (3)$$

where ρ ; the fluid density, t ; time, x_i ; the position vector in the ith coordinate direction, u_i ; the ith-fluid velocity component, B_i ; the component of the total body force per unit volume, p ; the local thermodynamic pressure.

$$\tau_{ij} = \mu\left[\left(\frac{\partial u_i}{\partial x_j} + \frac{\partial u_j}{\partial x_i}\right) - \frac{2}{3}\delta_{ij}\frac{\partial u_k}{\partial x_k}\right] \qquad (4)$$

Here, μ ; the dynamic viscosity of the fluid due to laminar diffusion, δ_{ij} ; the Kronecker delta function.

Algorithm and difference scheme

The code uses a finite-volume representation of the governing equations. Storm uses the PISO (Pressure Implicit with Splitting of Operators) algorithm developed by Issa (1985) and Issa et al. (1991) to solve the coupled system of governing equations. This method, part of a general class of implicit pressure-based solution techniques, employs a series of sequential operations at each time step in which the discrete momentum and pressure-based continuity equations are solved in an alternating 'predictor-corrector' fashion.

The solution algorithms chosen for the flow solver were LU decomposition for pressure and the Alternating Direction Implicit (ADI) method for all flow velocities. The convective terms in the governing equations were modeled using a second-order up-wind scheme which discrete using central differencing. The diffusive terms were modeled using an arithmetic mean interpolation scheme for evaluation of the transport coefficients between cell faces.

Model description

The model geometry and mesh are shown in Fig.17. From the specification of the target hybrid-sail, 2-D calculation was done in this paper. The coordinate and the definitions are defined as in the previous section. The flow domain of the model is 3.5C long in the X-direction, 2.3C long in the Y-direction as the representative length C that is the total sail chord. The flow domain was divided into 6 sections in the X-direction and 5 sections in the Y-direction. The mesh was stretched towards the sail to increase cell density near the sail and it contains 170 cells in the X-direction, 120 cells in the Y-direction for a total of 20400 cells.

Boundary and calculation conditions

The flow was computed by the laminar solution. No slip condition is given on the sail surface. The density calculation was based on the ideal gas law. The Reynolds number is 2.2×10^5 in the 8m/s on wind velocity as same as the experimental condition. The constant for 1.0×10^{-4} seconds at time interval was used and the duration time is 1.5~2 seconds in the calculation when a steady solution has been obtained.

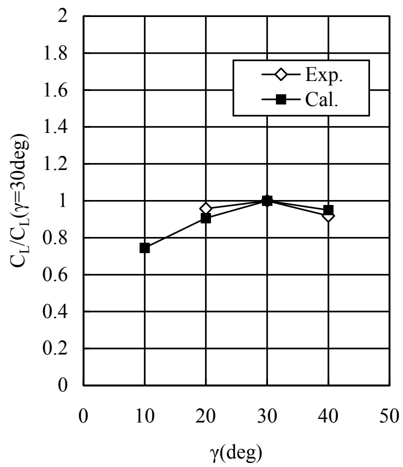

Fig.19 Comparison between the calculation results and the experimental ones on relative C_L when the boom angle is change (AR=2.34, α=20deg, β=35deg)

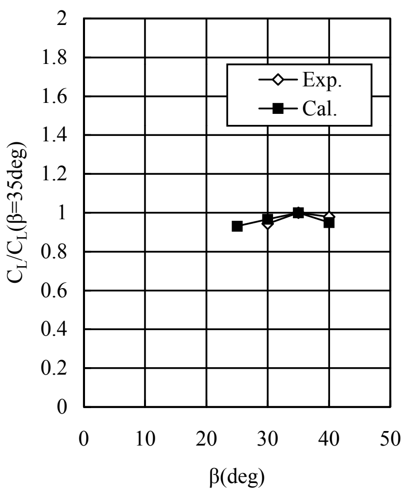

Fig.20 Comparison between the calculation results and the experimental ones on relative C_L when the slat angle is change (AR=2.34, α=20deg, γ=30deg)

Calculation results

The calculation results were compared with the experimental results as shown in Fig.18. The open diamonds stand for the experimental and the closed squares for calculation results in the figure. The calculation results are in the overestimation because the 3-dimensional effect of the sail and the bend of the soft sail are not considered in the calculation, but the trend between experimental results and calculation ones are coincided with each other.

The influence of the boom angle and the slat angle was investigated in the calculations. The results were compared with the experimental results in Fig.19 and Fig.20 by a relative evaluation. The maximum values are obtained in γ=30deg at Fig.19 and in β=35deg at Fig.20. The calculation is very useful to investigate the performance of the sail because the experimental results and calculation results have same trend on the maximum lift coefficient.

CONCLUTIONS

As the reference of the future work to build the sail-equipped motor ship, the aerodynamic characteristics of the square hybrid-sail were investigated experimentally and computationally. The results may be summarized as follows:

(1) The effectiveness of the present square hybrid-sail consisted of the rigid wing sail, which plays the role of a mast, the slat and the square soft sail was confirmed by comparing with the previous sails.

(2) The lift coefficient increases as the aspect ratio increases in the experiments. On the other hand, the drag coefficient is almost not change even if the aspect ratio is changed.

(3) The influence of the slat, the boom angle and the width of the soft sail on aerodynamic characteristics was investigated in the experiments. The maximum lift coefficient was obtained as 2.6 and the maximum thrust coefficient as 2.7 by the optimum setting of the sail.

(4) The aerodynamic characteristics were investigated in case that there is the gap between the rigid wing sail and the soft sail. The lift increases at the optimum setting more than the condition with no gap slightly though there is much possibility to decrease the lift in the others setting. It seems that the examination on the gap is necessary in the future research works.

(5) It was shown that the CFD calculation is very useful to investigate the performance of the hybrid-sail by a relative evaluation even if the sail has complex shape like this time.

REFERENCE

Abbott I.H. and Doenhoff A.E.V. (1959),"Theory of Wing Sections," *Dover Publications Inc.*

Adaptive Research (1997), http://www.adaptive-research.com or Fluid Technology Co. Ltd. in Japan, http://www.fluid.co.jp.

Issa R.I. (1985),"Solution of the Implicitly Discretized Fluid Flow Equations by Operator-Splitting," *Journal of Computational Physics*, Vol.62, pp40-65.

Issa R.I., Ahmadi-Befrui B., Beshay K.R. and Gosman A.D., (1991),"Solution of the Implicitly Discretized Reaching Flow Equations by Operator-Splitting," *Journal of Computational Physics*, Vol.93, pp388-410.

Hansen P.K.E. (2000), "Modarn Windships phase2, "*Danish Environmental Protection Agency,* http://www.mst.dk/udgiv/publications/2000/87-7944-019-3/html/default_eng.htm

Ishihara M., Watababe T. et al (1980),"Prospect of Sail-Equipped Motorship as Assessed from Experimental Ship 'Daioh',"*Shipboard Energy Conservation Symposium*, The Society of Naval Architects and

Marine Engineers, pp181-198.

Matsumoto N., Inoue M. and Sudo M. (1982),"Operating Performance of a Sail Equipped Tanker in Wave and Wind," *Second International Conference of Stability of Ships and Ocean Vehicles (STAB),* pp451-464.

Minami Y., Nimura T., Fujiwara T., Ueno M. (2003), "Investigation into Underwater Fin Arrangement Effect on Steady Sailing Characteristics of a Sail Assisted Ship, " *The Proceedings of the Thirteenth International Offshore and Polar Engineering Conference(ISOPE2003)*.

Usuki Iron Works Ltd.(1985),"International Voyage Sail-equipped Bulk Carrier 'USUKI PIONEER'," *Funenokagaku*, Vol.38, pp36-43. (in Japanese)